Colloid & Polymer Science Colloid Polym Sci 272:812–819 (1994)

Inner structure and properties of diamond-shaped and spherical α-Fe_2O_3 particles

K. Kandori, S. Tamura, and T. Ishikawa

School of Chemistry, Osaka University of Education, 4-88 Minamikawahori-cho, Tennoji-ku, Osaka, Japan

Abstract: Uniform diamond-shaped and spherical α-Fe_2O_3 particles, prepared by a forced hydrolysis of $FeCl_3$-HCl solutions, were characterized by various means. Electron microscope and x-ray diffraction measurements indicated that these particles are formed by recrystallization of β-FeOOH to α-Fe_2O_3 accompanying the dissolution of β-FeOOH. Ultramicropores were formed in spherical particles with outgassing in vacuo above 150 °C by dehydration of inner OH groups, proving that the particles are polycrystalline. On the other hand, the highly crystallized diamond-shaped particles showed a less microporosity and were thermally stable against outgassing up to 400 °C. These results are compatible with those obtained for the monodispersed cubic and spherical α-Fe_2O_3 particles reported in our previous paper [J Chem Soc Faraday Trans 87: 2241 (1991)].

Key words: Uniform particles – hematite – diamond-shaped particles – spherical particles – surface characterization

Introduction

The preparation of α-Fe_2O_3 particles uniform in shape with narrow size distribution such as spherical, cubic, ellipsoidal, etc. has been well studied [1–10]. Especially, Matijević and Scheiner prepared the uniform α-Fe_2O_3 particles by a forced hydrolysis of $FeCl_3$, $Fe(NO_3)_3$, and $Fe(ClO_4)_3$ solutions in 16 × 100 mm Teflon-lined screw-capped test tubes [3]. They found that the shape and size of the particles were influenced by the preparation conditions. Despite their extensive studies, little is known about the inner structure and property of the monodispersed α-Fe_2O_3 particles. In a previous paper [11], we characterized monodispersed spherical and cubic α-Fe_2O_3 particles produced following the recipe reported by Matijević and Scheiner [3], by gas adsorption and Fourier-transform infrared (FTIR) spectroscopy measurements, and then regarded that these monodispersed α-Fe_2O_3 particles are polycrystalline and constructed by an aggregation of fine ferric oxide hydroxide particles. However, the results were limited to the spherical and cubic particles with specific sizes. The study on the particles other than these particles is, therefore, of great importance for further understanding of the formation mechanism of the monodispersed α-Fe_2O_3 particles.

In general, not only the chemical parameters such as type of anions, acidity, and concentration of metal ions, but also the size and shape of reaction vessel, which probably affect the rate of heat conduction, are dominant factors for producing the monodispersed colloidal particles of metal oxides. The nucleation and growth of primary particles in the forced hydrolysis reaction are strongly susceptible to the rate of raising temperature at the first stage of the reaction. Hence, the shape and size of α-Fe_2O_3 particles can be expected to be influenced by the kinds of vessels used.

In this study, therefore, we carried out the forced hydrolysis of $FeCl_3$-HCl solution in the vessels differing from the test tube used in our previous study and the uniform idiomorphilic α-Fe_2O_3 particles precipitated were characterized by various techniques. The results of this study will yield insight into the inner structure of uniform α-Fe_2O_3 particles produced by the forced hydrolysis reaction of $FeCl_3$-HCl solution.

Experimental

1. Particle generation and characterization

Colloidal ferric compounds were prepared by aging $FeCl_3$-HCl solutions at elevated temperature. For this purpose, Pyrex glass vials (30 × 50 mm) containing the reacting solutions were tightly closed with Teflon-lined screw-caps and heated in a forced convention oven at 100 °C for 14 days. The concentrations of $FeCl_3$ and HCl in the starting solutions were systematically varied from 3.2×10^{-4} to 3.2×10^{-2} mol dm^{-3}, being much lower than the concentration of $FeCl_3$ in the study of Matijević and Scheiner ($1.8 \times 10^{-2} < [FeCl_3] < 5.0 \times 10^{-1}$ mol dm^{-3}) [3] while the concentration of HCl was nearly equal to their study ($1.0 \times 10^{-3} < [HCl] < 1.0 \times 10^{-1}$ mol dm^{-3}). The pH of the solutions after the reaction was below unity at room temperature. The settled particles were purified by dialysis against ion-exchanged and distilled water for ca. 2 weeks until no chloride ions were detected by $AgNO_3$ solution, and dried in an air oven at 70 °C for 16 h.

The particles thus obtained were characterized by transmission electron microscope (TEM), x-ray powder diffraction (XRD), gas adsorption of N_2 and H_2O, x-ray fluorescence spectroscopy (XFS), FTIR and zeta potential measurements in the manners as described in our previous papers [11, 12]. The zeta potential was measured in a Pen Kem microelectrophoresis instrument (Model 501) at a constant ionic strength of 1.0×10^{-4} mol dm^{-3} (KCl).

Results and discussion

1. Shape and size of precipitated particles

The size and shape of the particles, precipitated by a forced hydrolysis of $FeCl_3$-HCl solutions at 100 °C for 14 days in the screw-capped glass vials, strongly depended on the concentration of the reactants in the starting solution, especially on that of $FeCl_3$. Figure 1a gives the transmission electron micrographs of the precipitates at $FeCl_3$ and HCl concentration domains of greatest interest. The particle was never precipitated at $[FeCl_3] < 1.0 \times 10^{-3}$ mol dm^{-3}.

As can be seen in Fig. 1a, except for a system of $-\log[HCl] = 1.50$, the resulting particles turned from ellipsoidal to spherical via diamond with increase in $FeCl_3$ concentration, accompanying an enlargement of their sizes. On the other hand, Matijević and Scheiner did not prepare diamond-shaped particles by using test tubes, although they reported the formation of similar spherical and ellipsoidal α-Fe_2O_3 particles [3]. However, taking into account the difference of the concentration of Fe^{3+} ions in these two experiments, it is hard to define whether the diamond-shaped particles are a characteristic product of using the glass vials or not. On the other hand, Schwertzman and Cornell reported that the diamond-shaped particle formed on the forced hydrolysis of 2 dm^3 of a mixed solution of 2.0×10^{-2} mol dm^{-3} $Fe(NO_3)_3$ and 2.0×10^{-3} mol dm^{-3} HNO_3 in a Duran flask at 98 °C for 7 days [13]. To our knowledge, these diamond-shaped particles were the first successful production from $FeCl_3$ solutions. Since the purpose of this study is to characterize the uniform hematite particles, we focused on the diamond-shaped and spherical particles produced respectively at $-\log[FeCl_3] = 2.00$ and 1.50 under a fixed HCl concentration ($-\log[HCl] = 2.50$) because these particles are highly uniform in size and shape. It must be noted that the spherical particles of which diameter is 8 times larger than that of the spherical particles investigated in our previous paper [11] were employed in this study, because this will reveal some striking changes in the nature of spherical particles with their sizes.

The characteristic TEM pictures of the diamond-shaped and large spherical particles under investigation are displayed in Fig. 1b. It was ascertained from XRD measurements that both the spherical and diamond-shaped particles are formed by the phase transformation from β-FeOOH to α-Fe_2O_3. TEM observation also confirmed that the acicular β-FeOOH particles produced at the first stage of the reaction were dissolved and recrystallized to α-Fe_2O_3 after a certain aging period. The same phase transformation mechanism was reported for spherical and cubic α-Fe_2O_3 particles [3]. The complete transformation from β-FeOOH to α-Fe_2O_3 required 2 and 6 days, respectively, for the diamond-shaped and spherical particles. The mean length (l_d), mean diameter (d_s), chloride content and isoelectric point (iep) of the α-Fe_2O_3 particles formed by aging for 14 days are tabulated in Table 1.

2. *Characterization of diamond-shaped and spherical α-Fe_2O_3 particles*

Figure 2 delineates the change in zeta potential of the diamond-shaped and spherical particles in a 1.0×10^{-4} mol dm^{-3} KCl solution by pH. The positive surface charge is inverted to a negative one with increase in pH and the iep values are 5.5 and 5.0 for the diamond-shaped and spherical particles, respectively. Recently, we reported the pronounced effects of residual chloride ions on the surface charge of the cubic α-Fe_2O_3 particles produced by a forced hydrolysis of a 0.1 mol dm^{-3} $FeCl_3$ solution [12]; the chloride ions, of which the molar ratio to ferric ions was 1.0×10^{-3}, are preferentially located within the surface region of the particles to induce a high surface acidity giving the iep around pH 3.0 and were hardly removed by repetition of washing with KOH solution and distilled water. Although the diamond-shaped and spherical particles produced in this study possess similar total amounts of

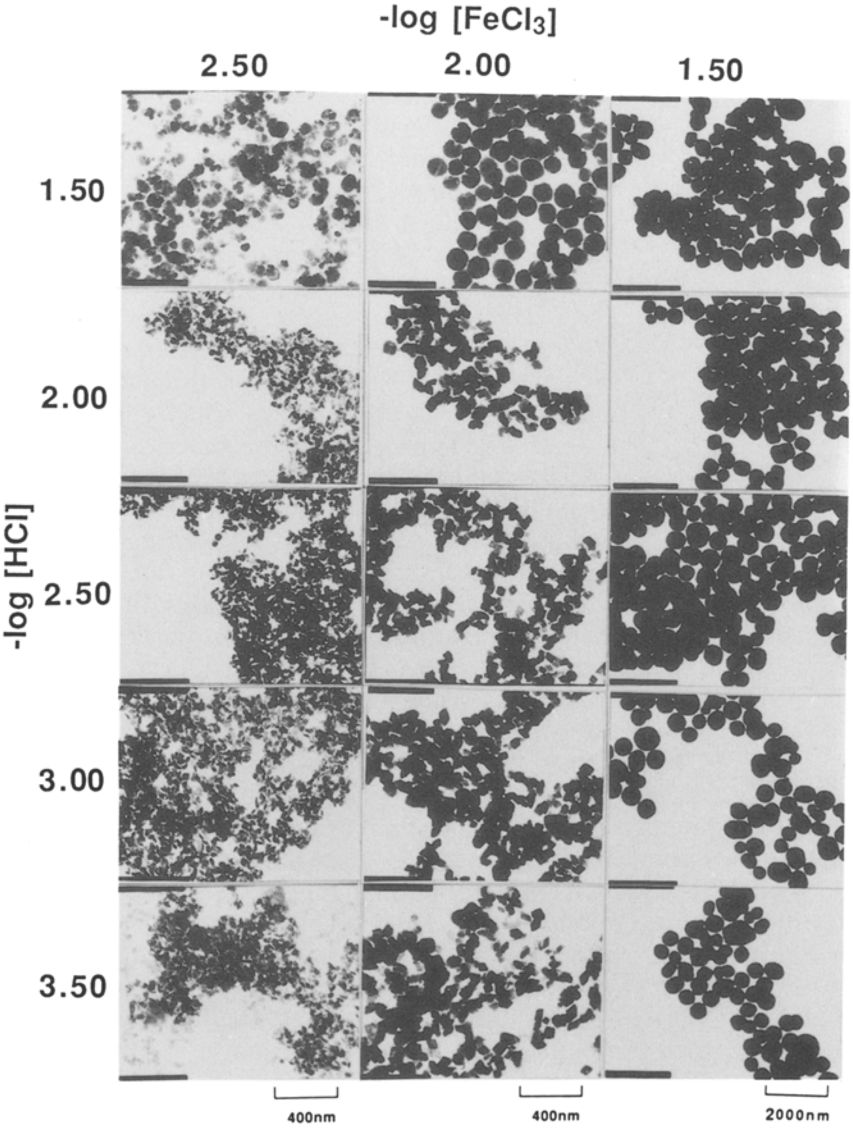

Fig. 1a. Electron micrographs of precipitates. Note that the magnifications are different.

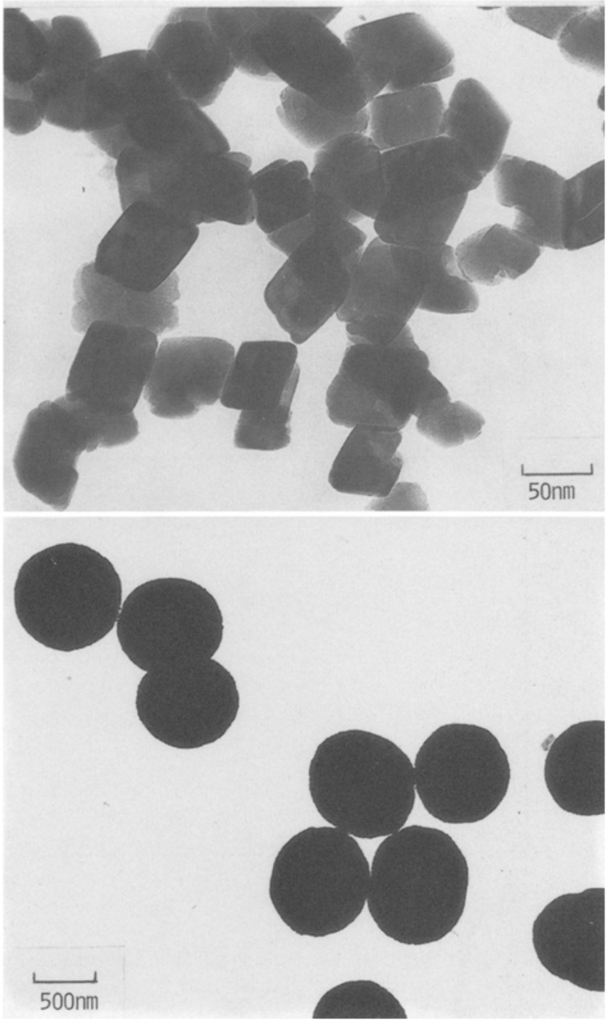

Fig. 1b. Electron micrographs of diamond-shaped and spherical hematite particles

chloride ions (Table 1), the iep values of these particles are higher than that of the cubic ones prepared in the previous study, suggesting that chloride ions are not highly concentrated on the surface of the particles prepared in this study.

The adsorption isotherms of N_2 on the diamond-shaped and spherical α-Fe_2O_3 particles treated at various outgassing temperatures are shown in Figs. 3(a) and (b), respectively. The N_2 adsorption isotherms on the diamond-shaped particles belong to Type II in the BDDT classification and no remarkable change with outgassing temperature was observed. On the other hand, the adsorption isotherms on the spherical particles outgassed between 100 and 200 °C belong to Type I while the amount of N_2 adsorbed for the particles outgassed above 300 °C drastically decreased and gave Type III adsorption isotherms, indicating that the microporosity of the spherical particles developed in the low outgassing temperature region. Similar change was observed in the adsorption isotherms of H_2O on these particles as is shown in Fig. 4, although the isotherms on the diamond-shaped particles outgassed at 300° and 400 °C showed slightly larger amounts of H_2O adsorbed. Then we assessed the micropore structure by the *t*-plot analysis of the N_2 adsorption isotherms as shown in Fig. 5. The *t*-plots of the diamond-shaped particles curved without distinct reflecting point, implying the existence of micropores with different sizes. The micropore analysis (MP) method [14] gives the distribution of micropores diameter from 1.6 to 2.4 nm, anticipating the interstices among primary particles. On the other hand, the finding that the *t*-plots of the spherical samples outgassed between 100° and 200 °C clearly bent at a thickness of 0.4 nm is

Table 1. Sizes, chloride contents and iep of uniform diamond shaped and spherical hematite particles produced by aging for 14 days

	Size (nm)	Chloride content Cl/Fe molar ratio	iep
	l_d		
Diamond shaped	70 ± 8	6.6×10^{-4}	5.5
	d_s		
Spherical	820 ± 84	1.6×10^{-3}	5.0

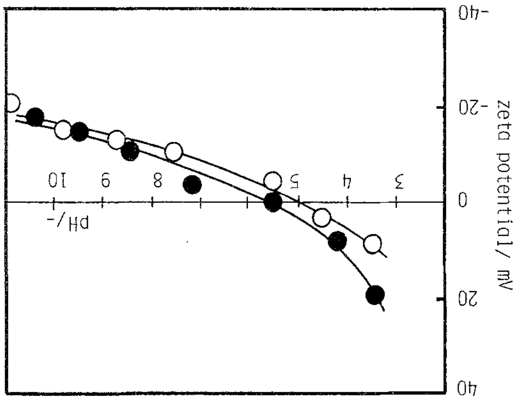

Fig. 2. Change in zeta potential of (●) diamond-shaped and (○) spherical particles

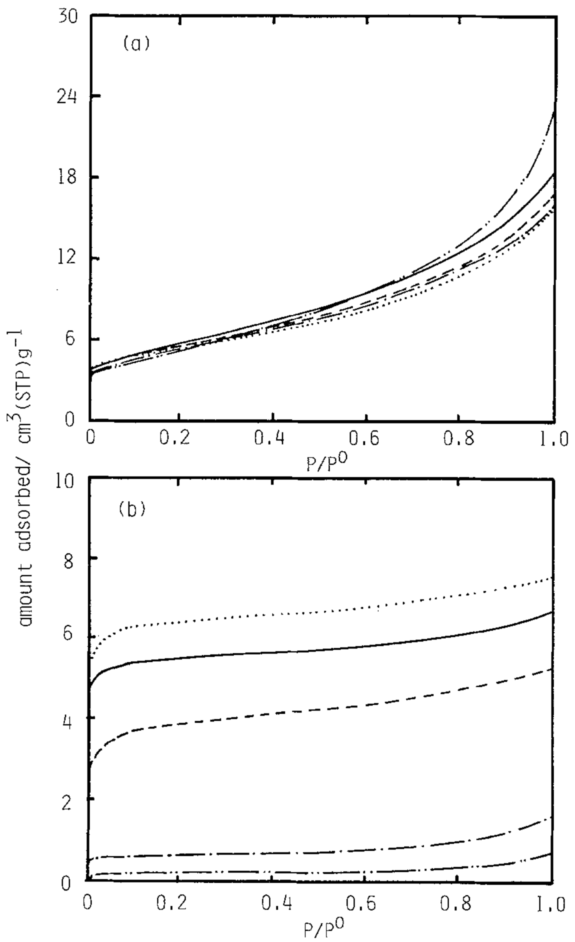

Fig. 3. N_2 adsorption isotherms at various outgassing temperatures on a) diamond-shaped and b) spherical particles. Outgassing temp./°C: (——) 100; (··· ···) 150; (----) 200; (–·–) 300; (–··–) 400

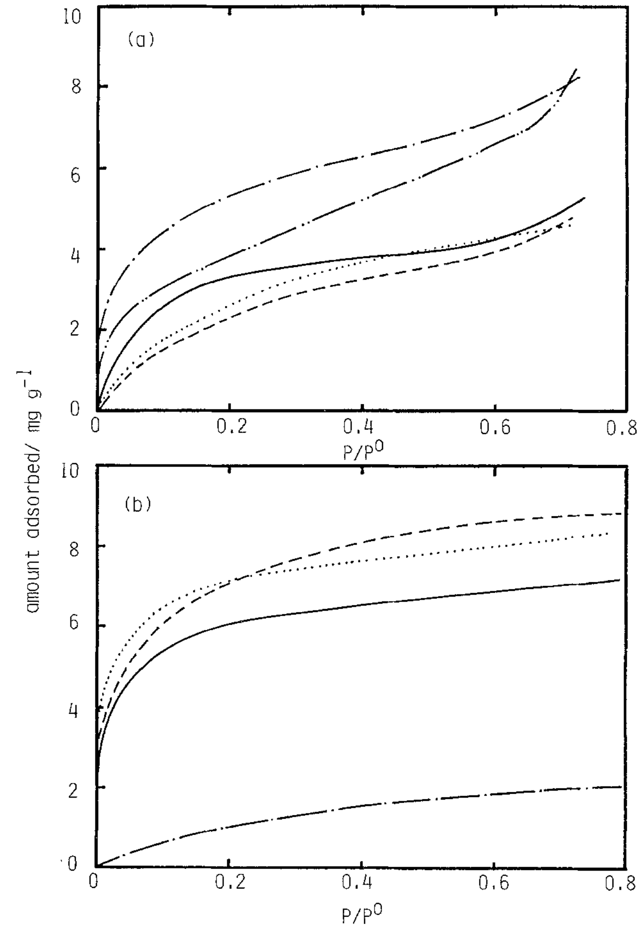

Fig. 4. H_2O adsorption isotherms at various outgassing temperatures on a) diamond-shaped and b) spherical particles. Outgassing temp./°C: (——) 100; (··· ···) 150; (----) 200; (–·–) 300; (–··–) 400

indicative of the existence of micropores with a width of 0.8 nm. Interestingly, the similar uniform slit-shaped micropores of a 0.8 nm width are formed in plate-like δ-FeOOH particles by treatment between 150° and 200 °C in vacuo [15].

In the course of studying the microporosity of the particles, the specific surface areas (S_n and S_w) calculated from N_2 and H_2O adsorption isotherms, respectively, are listed in Table 2 along with the specific surface area (S_g) calculated from their particle sizes assuming that the density of α-Fe_2O_3 is 5.26 g cm^{-3} [16]. Here, S_g values listed in Table 2 for each particle are the values before the heat treatment in vacuo, because the morphology of the particles did not change by the pretreatment. S_n and S_w were evaluated using the BET equation taking the molecular cross-sectional areas of N_2 and H_2O to be 0.162 and 0.108 nm^2, respectively. These surface areas can be used for a quantitative discussion of the porosity. On the spherical particles, both S_n and S_w are larger than the corresponding S_g and decrease with increasing the outgassing temperature, while S_w/S_n ratio increased up to 3.8. This shows that the ultramicroporosity of the spherical particles progressed with raising the outgassing temperature, because the S_w/S_n ratio is a measure of the fraction of ultramicropores which are accessible to H_2O molecules but not to N_2 ones. On the other hand, S_w of the diamond-shaped particles decreased up to 200 °C and increased again at 300 °C followed by a reduction at 400 °C, though S_n showed to be

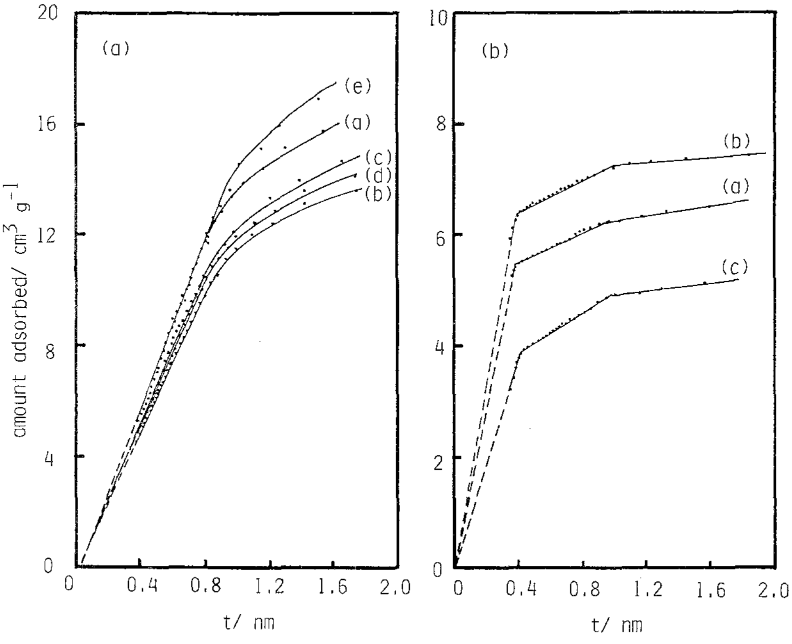

Fig. 5. t-plots for a) diamond-shaped and b) spherical hematite particles. Pretreatment temp./°C: a) 100; b) 150; c) 200; d) 300; e) 400

Table 2. Various specific surface areas ($m^2 g^{-1}$) obtained from N_2 adsorption (S_n), H_2O adsorption (S_w) and particle size (S_g)

Outgassing temp./°C	Diamond shaped				Spherical			
	S_n	S_w	S_w/S_n	S_g1)	S_n	S_w	S_w/S_n	S_g1)
100	20.4	11.0	0.5	18.1	19.5	31.2	1.6	1.4
150	18.5	6.8	0.4	18.1	22.7	40.0	1.8	1.4
200	19.5	6.2	0.3	18.1	14.0	40.8	2.9	1.4
300	19.0	13.5	0.7	18.1	2.1	8.0	3.8	1.4
400	18.9	8.7	0.5	18.1	0.8	–	–	1.4

1) All the values for each particle are calculated from their particle sizes before heat treatment in vacuo by assuming the density of the particle is 5.26 $g cm^{-3}$.

almost constant over the entire outgassing temperature. This result indicates that few ultramicropores were generated by treating at 300 °C but they were sintered at 400 °C. Such discrepancy for the spherical and diamond-shaped particles can be accounted for by the difference in their crystallinities; the dehydration reaction forming the ultramicropores takes place more seldom in the well crystalline diamond-shaped particles as compared to the less crystalline spherical ones. In fact, a highly crystalline particle with a diameter of 128 nm gave the S_w/S_n values of ca. unity over the entire outgassing temperature range from 100° to 400 °C, as well as the spherical shape particles reported in a previous paper [11]. It should be emphasized that S_n approximates to S_g and is less than S_w at all outgassing temperatures for the diamond-shaped particles. It appears therefore that the particles are appreciably non-porous and their surfaces are hydrophobic. This hydrophobicity of the diamond-shaped particles may be associated with the small number of surface adsorption sites of H_2O such as surface hydroxyl groups, because these particles showed less weight loss by heating as described below.

Figure 6 illustrates the FTIR spectra of the diamond-shaped and spherical particles in the OH stretching vibration region. These spectra were recorded in vacuo at room temperature after heating in vacuo at different temperatures for 2 h. Strong absorption bands appeared at maximum wavenumber ca. 3430 and ca. 3400 cm^{-1} on the

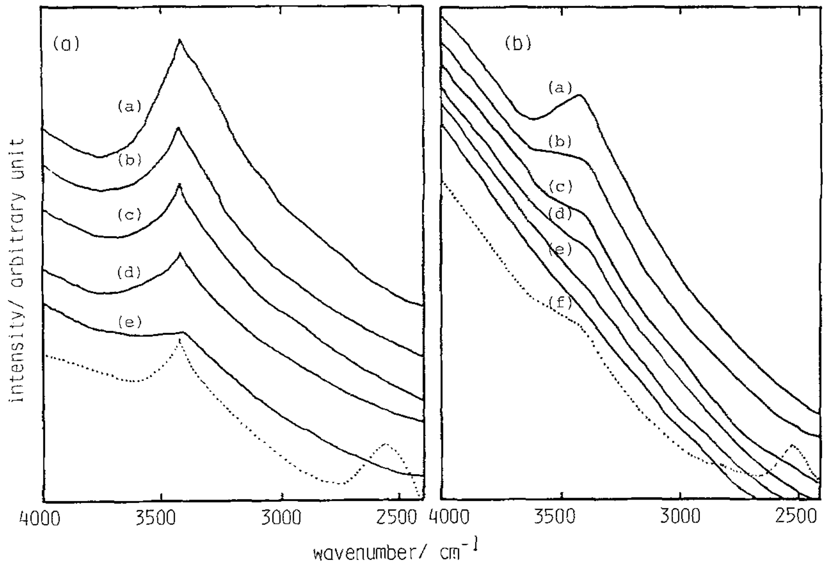

Fig. 6. FTIR spectra of a) diamond-shaped and b) spherical hematite particles. Outgassing temp./°C a) 25; b) 100; c) 150; d) 200; e) 300; f) 400. The dotted lines were measured after exchanging with D_2O for four cycles.

diamond-shaped and spherical particles, respectively. We previously found similar peaks in the case of the spherical and cubic monodispersed particles and assigned these bands to the inner OH groups from analogy to the spectra of β-FeOOH particles [11]. Therefore, the 3430 and 3400 cm^{-1} bands observed in the present study can be attributed to the inner OH groups. To gain unambiguous evidence for this assignment, the ^1H–^2H exchange was performed by repetition of the adsorption-desorption cycle of heavy water. During this deuteration, new small bands grew at 2550 and 2530 cm^{-1} for the diamond-shaped and spherical particles, respectively, as depicted by dotted lines in Fig. 6. The isotope ratios ν_{OH}/ν_{OD} (3430/2550 = 1.345 and 3400/2530 = 1.344) are close to the theoretical value of 1.374, proving that these bands are assignable to the stretching vibration of OH groups. Rochester and Topham have found a similar broad band at 3440 cm^{-1} for the hematite particles prepared from a dehydration of α-FeOOH particles in oxygen atmosphere above 300 °C, and assigned it to bulk or surface OH groups [17]. Since only a small portion of the 3430 and 3400 cm^{-1} bands observed in the present study showed an isotope shift (Fig. 6), these bands can be assigned to the bulk OH groups. The surface OH band should appear around 3640 cm^{-1} as was reported by Blyholder and Richardson [18], but this cannot be confirmed because of the small specific surface area and/or small number of surface OH groups of these particles as ascertained in the foregoing paragraph. The absorbances of the inner OH bands at 3430 and 3400 cm^{-1} decreased on raising outgassing temperature, while the weight loss by heating in vacuo increased. The relation between weight loss and absorbance is given by a partial linear relationship as is shown in Fig. 7. Thus the weight loss would be mainly due to the dehydration of the inner OH groups producing ultramicropores.

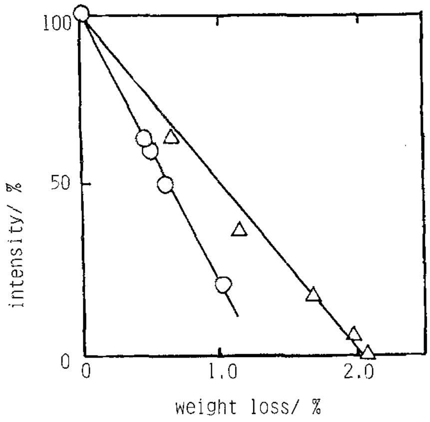

Fig. 7. Relationship between the absorbance of the inner OH stretching bands and weight loss: ○, diamond-shaped, △, spherical

The results of gas adsorption and FTIR measurements obtained in this study suggest that the α-Fe_2O_3 particles produced by a forced hydrolysis of $FeCl_3$-HCl solutions are polycrystalline. However, understanding of their detailed structure must await more experimentation.

Acknowledgments

The authors are indebted to Dr. Yoshihira Okanda and Dr. Masao Fukusumi of Osaka Municipal Technical Research Institute for their help in the TEM measurement. Special thanks are due to Mrs. Kyoko Suganuma of Chemilite Industry Co. for the x-ray fluorescence spectroscopy. This work was supported in part by the Science Research Fund of the Ministry of Education of the Japanese Government.

References

1. Matijević E (1986) Langmuir 2:12
2. Matijević E (1985) Ann Rev Mater Sci 15:483
3. Matijević E, Scheiner P (1978) J Colloid Interface Sci 63:509
4. Kally N, Matijević E (1985) Colloid Surf 13:145
5. Matijević E, Cimas S (1987) Colloid Polym Sci 265:155
6. Kratohvil S, Matijević E, Ozaki M (1984) Colloid Polym Sci 262:804
7. Ozaki M, Kratohvil S, Matijević E (1984) J Colloid Interface Sci 102:146
8. Hamada S, Niizeki S, Kudo Y (1986) Bull Chem Soc Jpn 59:3443
9. Joekes I, Galembeck F, Santos HS, Jafelicci M Jr (1981) J Colloid Interface Sci 84:278
10. Hamada S, Matijević E (1982) J Chem Soc Faraday Trans 1 78:2147
11. Kandori K, Kawashima Y, Ishikawa T (1991) J Chem Soc Faraday Trans 87:2241
12. Kandori K, Kawashima Y, Ishikawa T (1993) J Materials Sci Letter 12:288
13. Schwerzmann U, Cornell RM (1991) In: "Iron Oxides in the Laboratory," VCH New York p. 102
14. Mikhail RH, Brunauer S, Bodor EE (1968) J Colloid Interface Sci 26:45
15. Ishikawa T, Cai WY, Kandori K (1992) J Chem Soc Faraday Trans 88:1173
16. ASTM Cards No. 24–72.
17. Rochester CH, Topham SA (1979) J Chem Soc Faraday Trans 1 75:1073
18. Blyholder G, Richardson EA (1962) J Phys Chem 66:2599

Received November 17, 1992;
accepted September 7, 1993

Authors' address:

Kazuhiko Kandori
School of Chemistry
Osaka University of Education
4-698-1 Asahigaoka
Kashiwara-shi
Osaka 582, Japan